

Supporting information for:

## Improved conductivity of $\text{NdFeO}_3$ through partial substitution of Nd by Ca: a theoretical study

You Wang,<sup>a</sup> Yun Wang,<sup>b</sup> Wei Ren,<sup>c</sup> Porun Liu,<sup>b</sup> Huijun Zhao,<sup>\* b</sup> Jun Chen,<sup>a</sup> Jinxia  
Deng<sup>d</sup> and Xianran Xing<sup>\* a</sup>

a. Department of Physical Chemistry, University of Science and Technology Beijing, Beijing 100083, China,

b. Centre for clean Environment and Energy and Griffith School of Environment, Griffith University, Gold Coast Campus, QLD  
4222, Australian

c. Department of Physics, International Center of Quantum and Molecular Structures, and Materials Genome Institute, Shanghai  
University, Shanghai 200444, China

d. Department of Chemistry, University of Science and technology Beijing, Beijing 100083, China

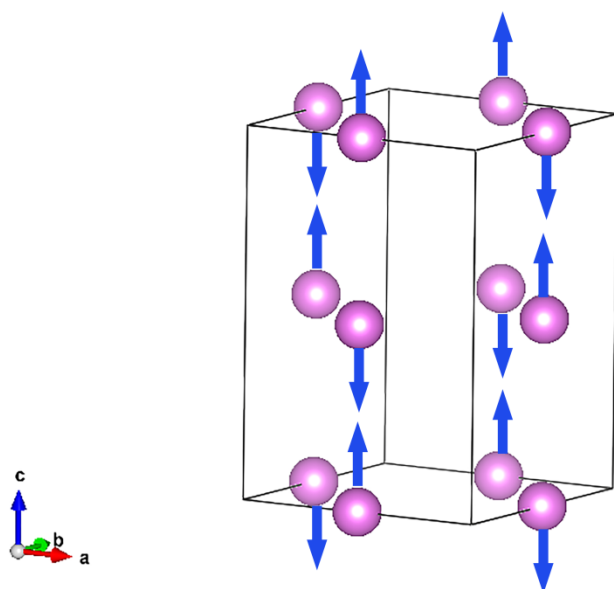


Fig. S1 The G-type antiferromagnetic structure of  $\text{NdFeO}_3$ .

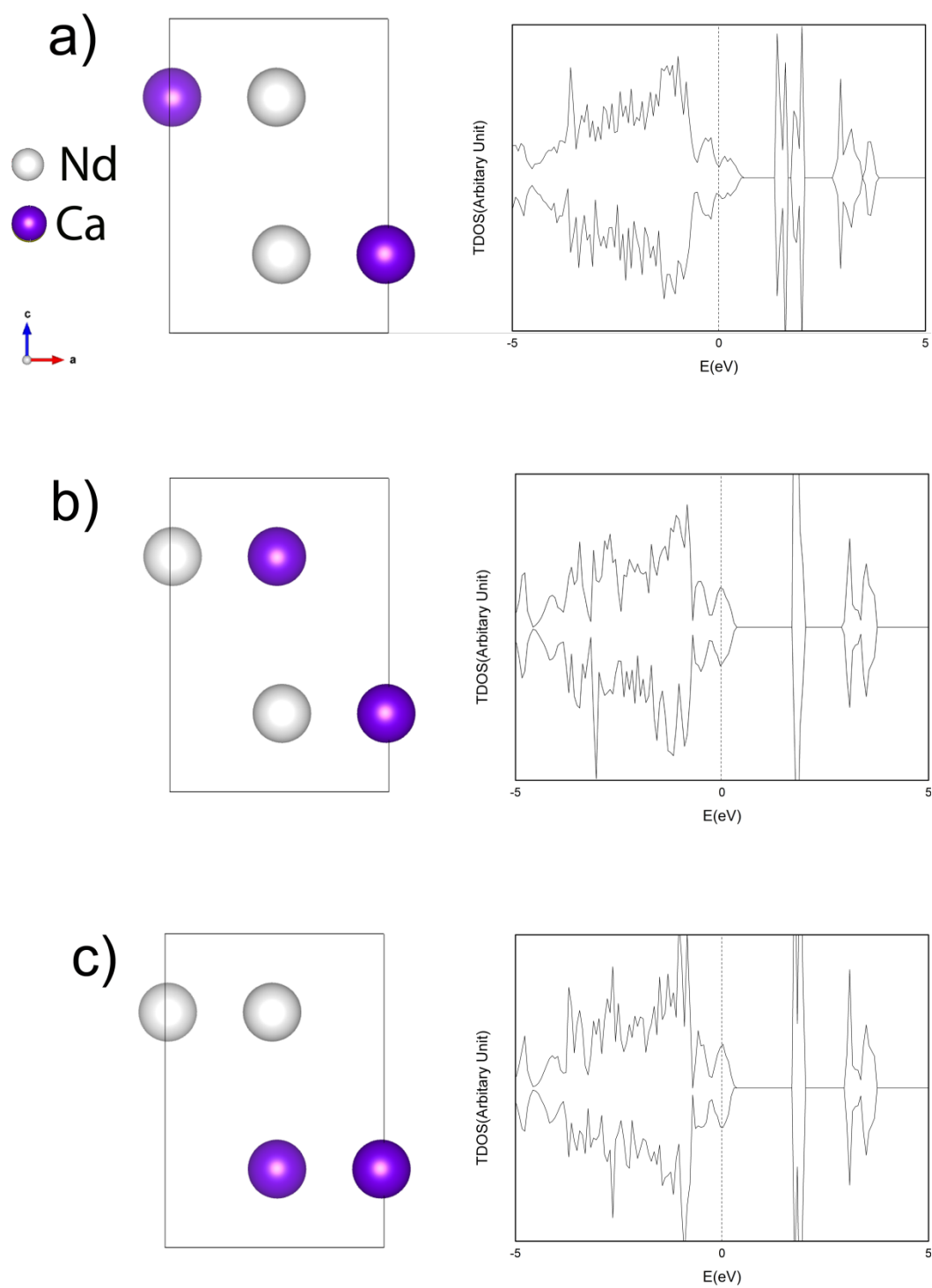


Fig. S2 Three types of Nd/Ca arrangements and their total density of states of  $\text{Nd}_{0.5}\text{Ca}_{0.5}\text{FeO}_3$ . For clarity, we only show the arrangements of Nd and Ca from the supercell structures.

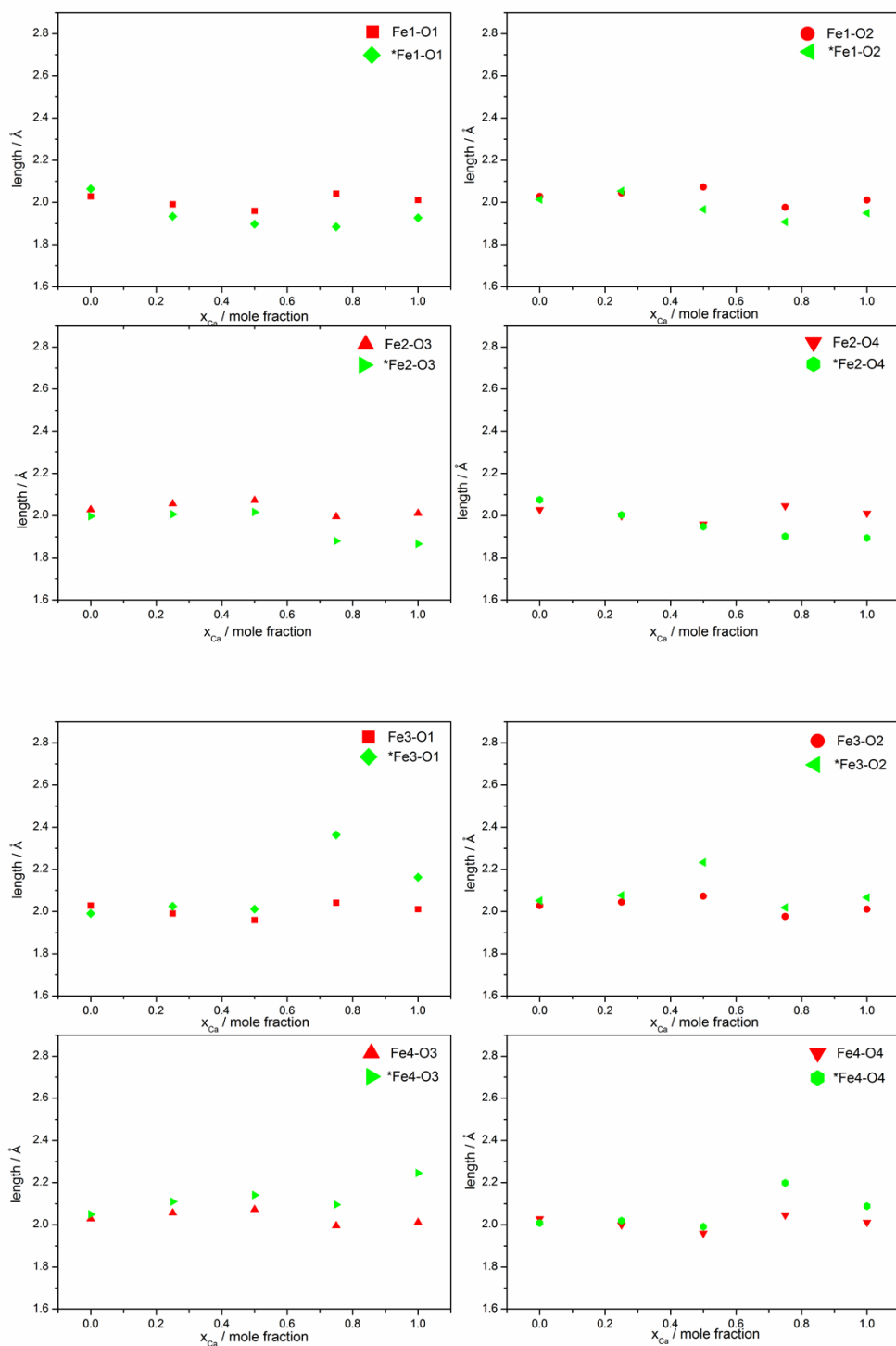
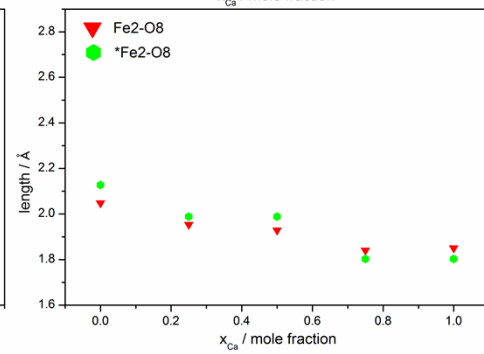
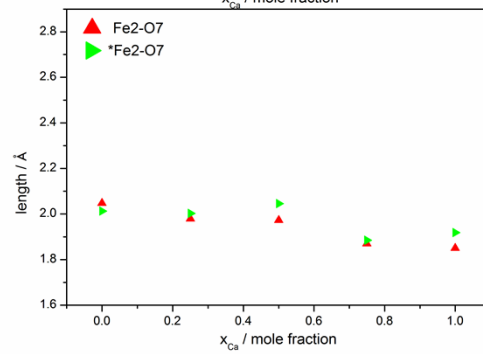
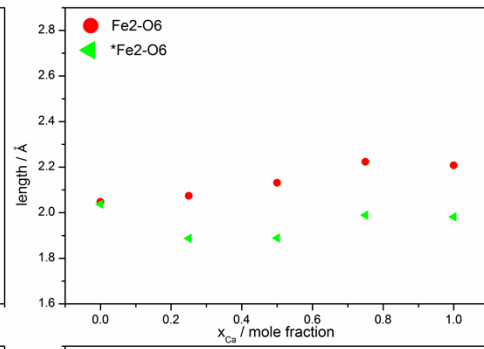
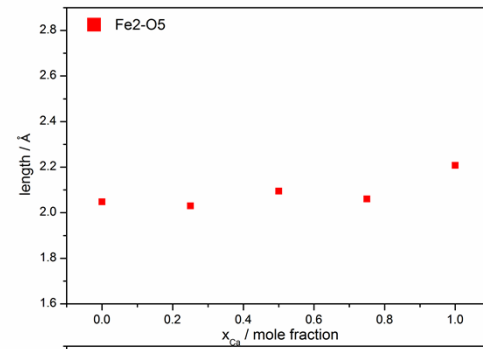
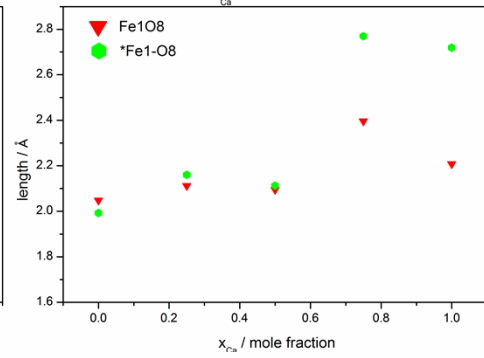
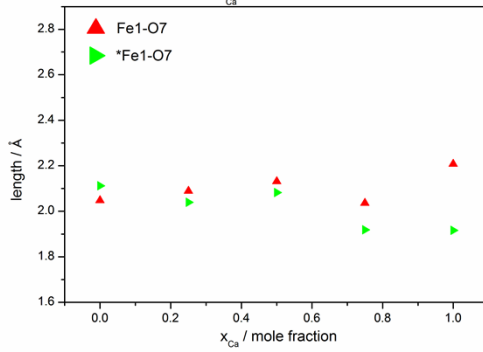
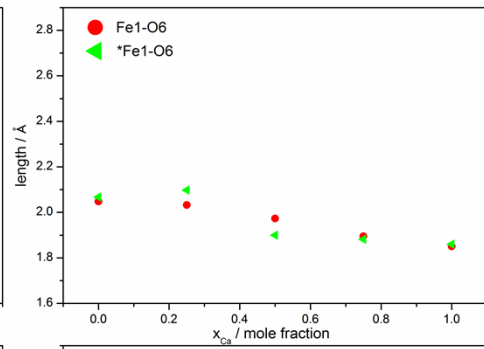
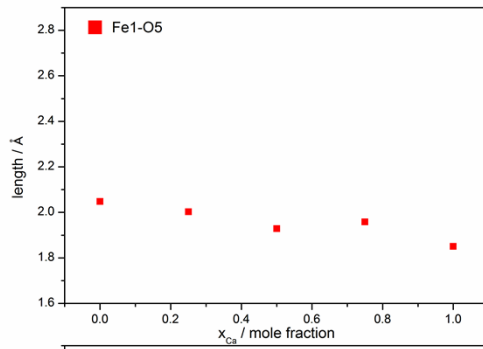


Fig. S3 The axial Fe-O bond length (Å) for  $Nd_{1-x}Ca_xFeO_3$  (red) and  $Nd_{1-x}Ca_xFeO_{2.75}$  (green) ( $x=0.00, 0.25, 0.50, 0.75, 1.00$ ). See Fig. S7 for the numbering of Fe and O ions.



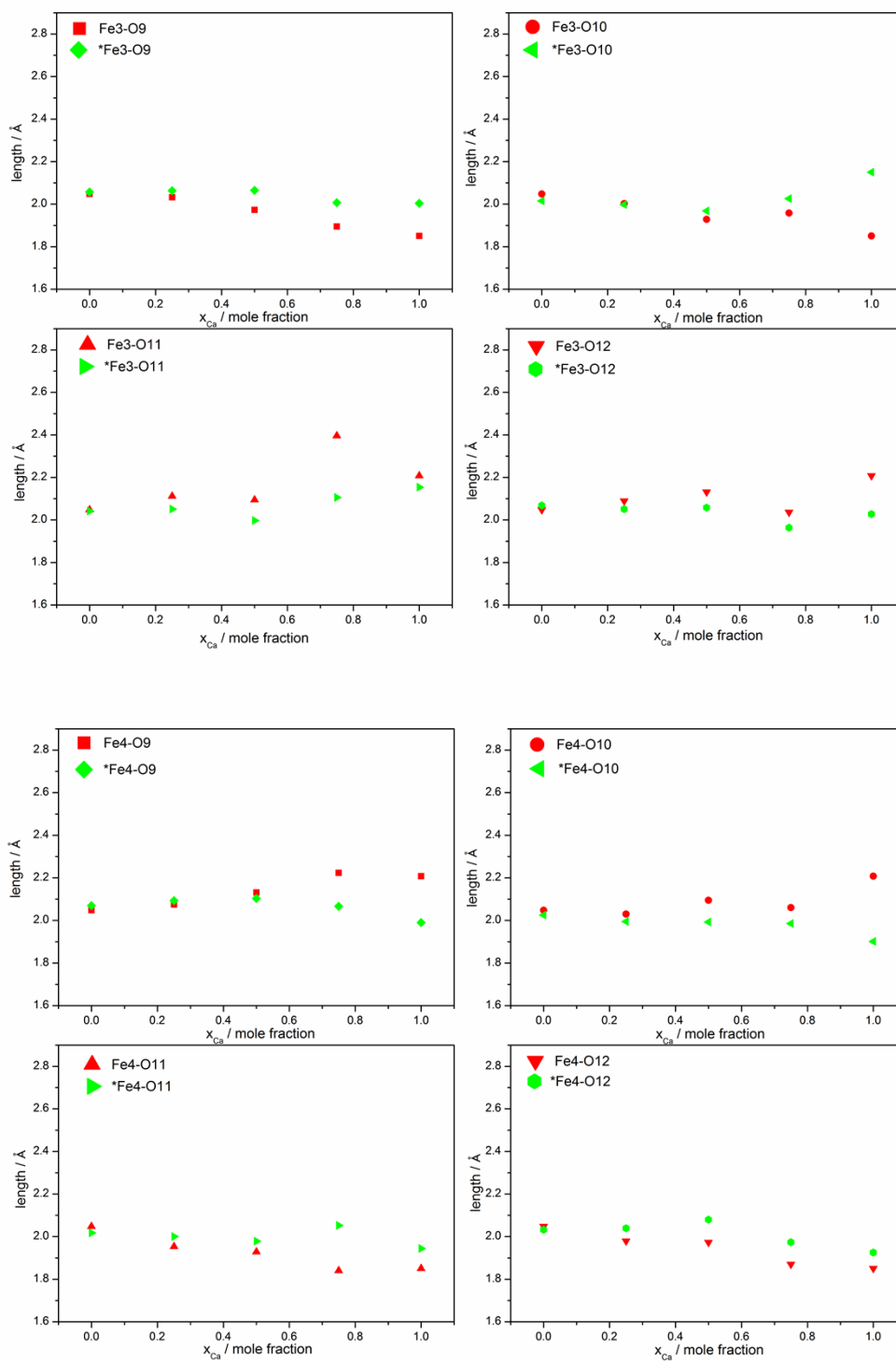


Fig. S4 The equatorial Fe-O bond length (Å) for Nd<sub>1-x</sub>Ca<sub>x</sub>FeO<sub>3</sub> (red) and Nd<sub>1-x</sub>Ca<sub>x</sub>FeO<sub>2.75</sub> (green) (x=0.00, 0.25, 0.50, 0.75, 1.00).

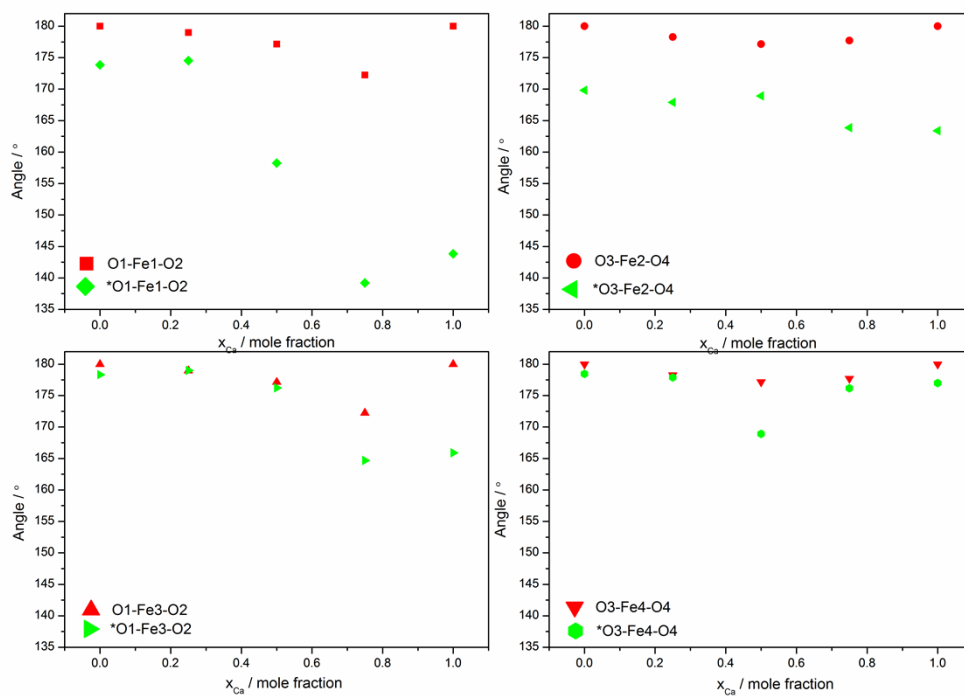


Fig. S5 The axial O-Fe-O bond angle ( $^{\circ}$ ) for  $Nd_{1-x}Ca_xFeO_3$  (red) and  $Nd_{1-x}Ca_xFeO_{2.75}$  (green) ( $x=0.00, 0.25, 0.50, 0.75, 1.00$ ).

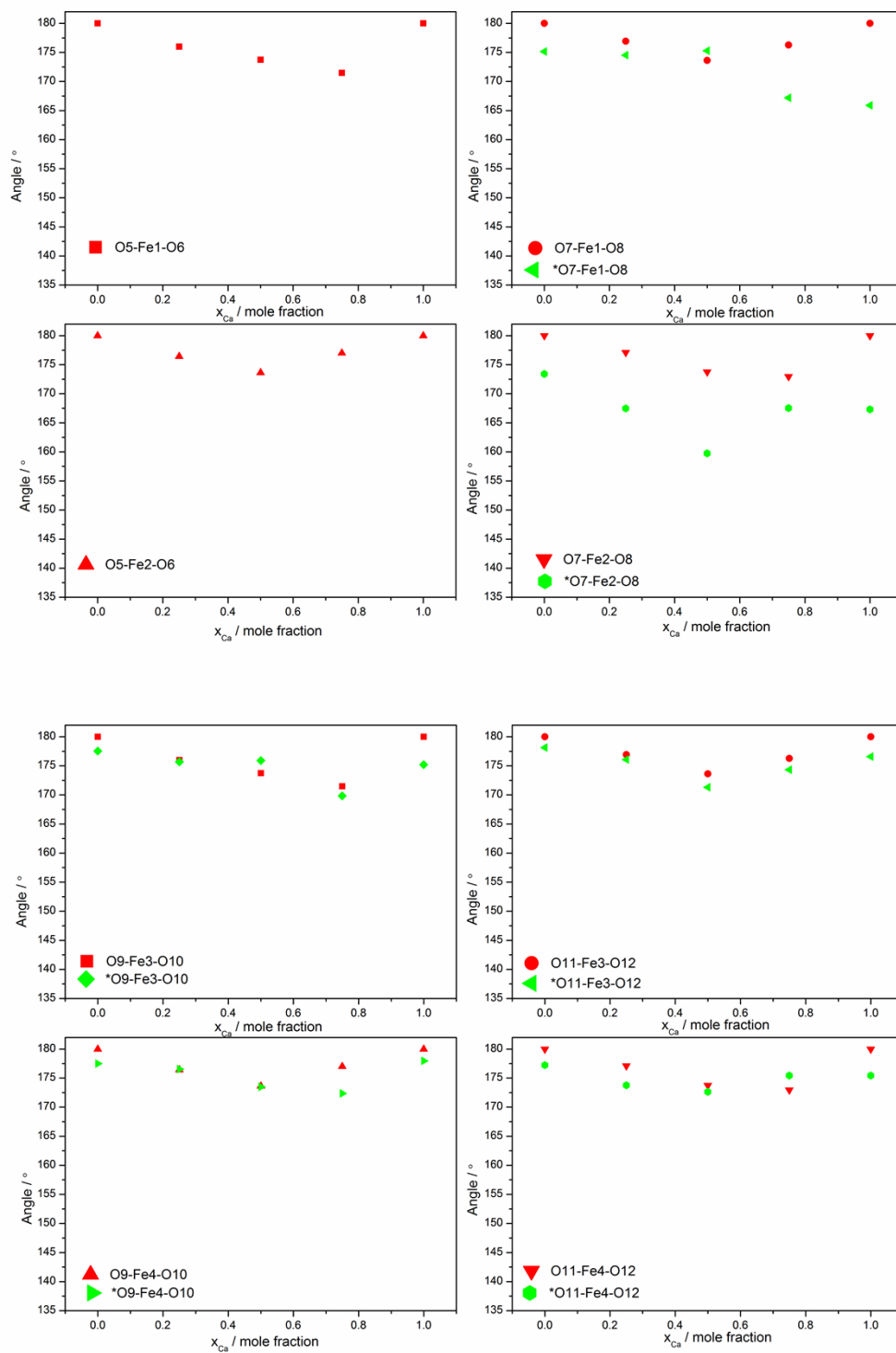


Fig. S6 The equatorial O-Fe-O bond angle (°) for  $Nd_{1-x}Ca_xFeO_3$  (red) and  $Nd_{1-x}Ca_xFeO_{2.75}$  (green) ( $x=0.00, 0.25, 0.50, 0.75, 1.00$ ).

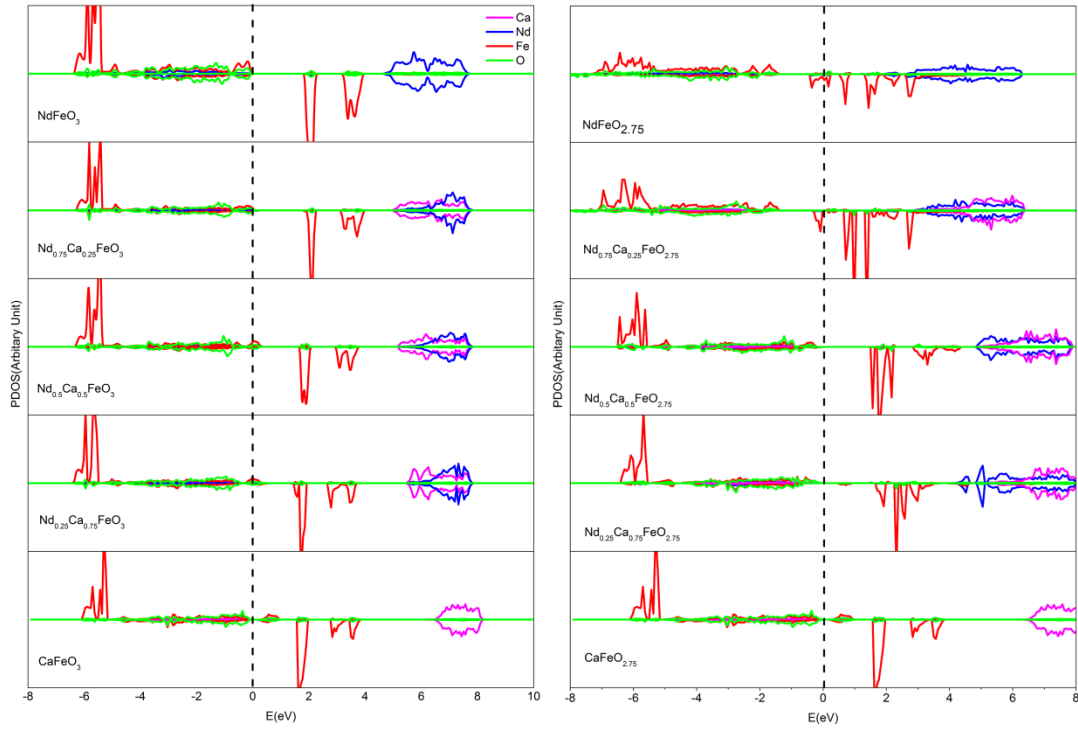


Fig. S7 Partial density of states (PDOS) of  $\text{Nd}_{1-x}\text{Ca}_x\text{FeO}_3$  ( $x=0.00, 0.25, 0.50, 0.75$  or  $1.00, \delta=0.00$  or  $0.25$ ).

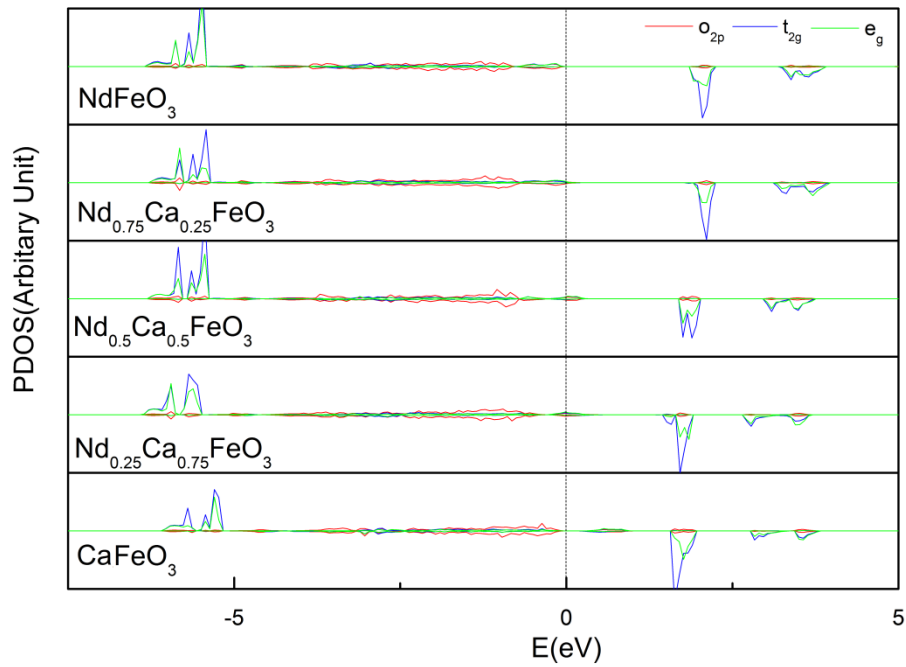


Fig. S8 The PDOS images of O  $2p$ , Fe  $t_{2g}$  and Fe  $e_g$  are shown for the structures of  $\text{Nd}_{1-x}\text{Ca}_x\text{FeO}_3$  ( $x=0.00, 0.25, 0.50, 0.75$  and  $1.00$ ).



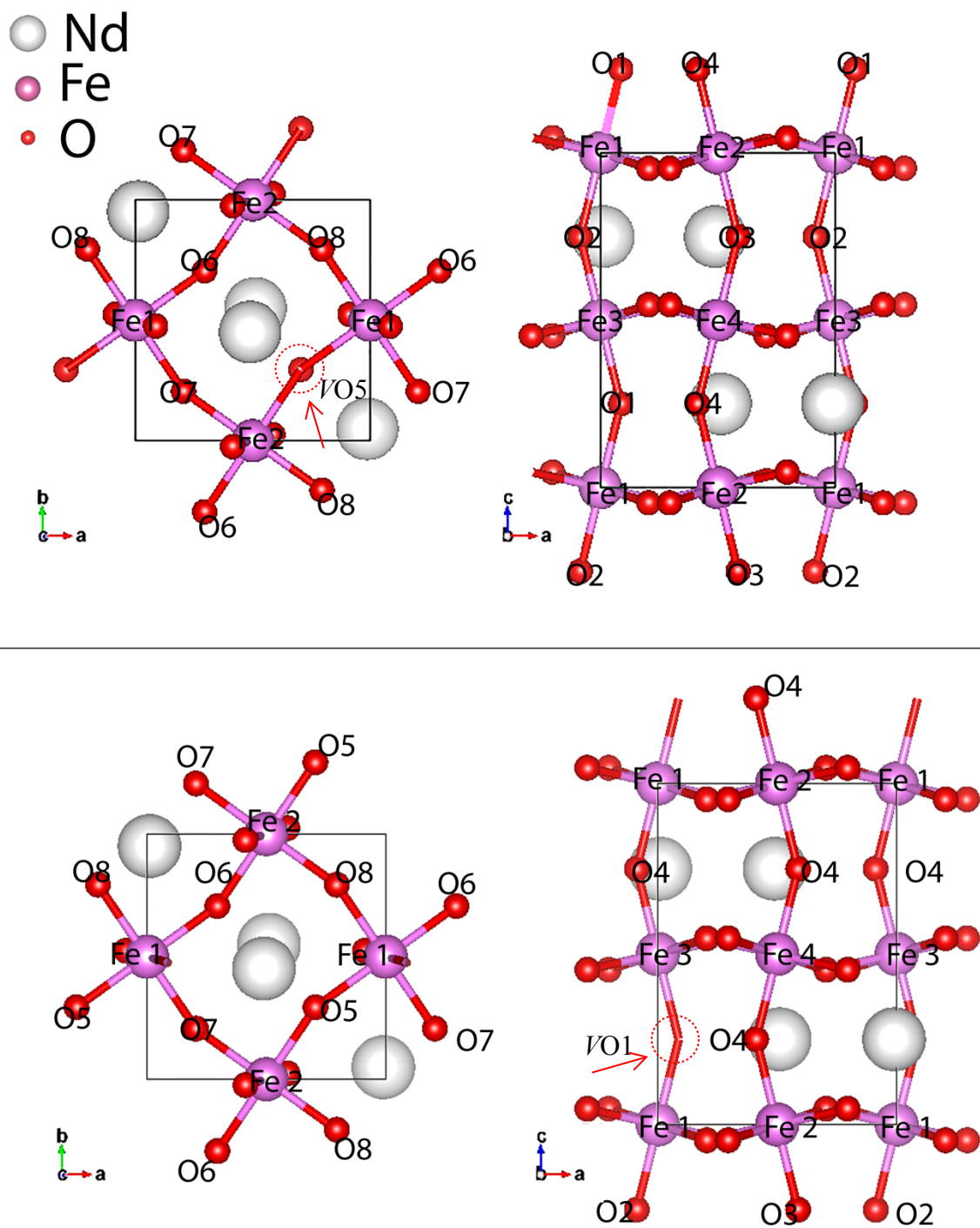


Fig. S9 Top views and side views of NdFeO<sub>2.75</sub>. Oxygen vacancies formed along axial Fe-O-Fe bond (lower) and equatorial (upper). Structures are visualized with VESTA.